STATE OF THE ART IN ZONE MODELING OF FIRES

by

Walter W. Jones
Building and Fire Research Laboratory
National Institute of Standards and Technology
Gaithersburg, MD 20899 USA

Reprinted from the Vereinigung zur Forderung des Deutschen Brandschutzes e.V. (VFDB). International Fire Protection Seminar, 9th. Engineering Methods for Fire Safety. Proceedings. May 25-26, 2001, Munich, Germany, A.4/89-126 pp, 2001. ISBN 3-89288-133-2.

National Institute of Standards and Technology
Technology Administration, U.S. Department of Commerce

State of the Art in Zone Modeling of Fires*

Walter W. Jones

National Institute of Standards and Technology
9th International Fire Protection Seminar, Munich
May 25 and 26, 2001

Abstract

This paper discusses the current capabilities of zone fire modeling. CFAST is used as the example, but as discussed at the end, the fundamental concepts are applicable to a wide range of models, available around the world. While there are aspects of the current model such as horizontal smoke movement that are features of CFAST, the basic conservation equations, methods of solution and difficulties are common to the whole spectrum of this class of building system models.

Overview

Analytical models for predicting fire behavior have been evolving since the 1960's. Over the past decade, the completeness of the models has grown considerably. In the beginning, the focus of these efforts was to describe in mathematical language the various phenomena which were observed in fire growth and spread. These separate representations have typically described only a small part of a fire. When combined though, they can create a complex computational model intended to give an estimate of the expected course of a fire based upon given input parameters. These analytical models have progressed to the point of providing predictions of fire behavior with an accuracy suitable for most engineering applications. In a recent international survey [1], 36 actively supported models were identified. Of these, 20 predict the fire driven environment (mainly temperature) and 19 predict smoke movement in some way. Six calculate fire growth rate, nine predict fire endurance, four address detector or sprinkler response, and two calculate evacuation times. The computer models now available vary considerably in scope, complexity, and purpose. Simple “compartment filling” models such as the Available Safe Egress Time (ASET) model [2] run quickly on almost any computer, and provide good estimates of a few parameters of interest for a fire in a single compartment. A special purpose model can provide a single function. For example, COMPF2 [3] calculates post-flashover compartment temperatures and LAVENT [4] includes the interaction of ceiling jets with fusible links in a compartment containing ceiling vents and draft curtains.

In addition to the single-compartment models mentioned above, there are a smaller number of multi-compartment models which have been developed. These include the BRI transport model [5], FAST [6], CCFM [7] and the CFAST model discussed below [8].

Although the papers are several years old, Mitler [9] and Jones [10] reviewed the underlying physics in several of the fire models in detail. The models fall into two categories: those that start

* The translation into German has been omitted from this printing

with the principles of conservation of mass, momentum, and energy such as CFAST; and those that typically are curve fits to particular experiments or series of experiments, used in order to discern the underlying relationship among some parameters. In both cases, errors arise in those instances where a mathematical short cut was taken, a simplifying assumption was made, or something important was not well enough understood to include.

The environment in a fire is constantly changing. Thus the equations are usually in the form of *differential equations*. A complete set of equations can compute the conditions produced by the fire at a given time in a specified volume of air. Referred to as a *control volume*, the model assumes that the predicted conditions within this volume are uniform at any time. Thus, the control volume has one temperature, smoke density, gas concentration, *etc*.

Different models divide the building into different numbers of control volumes depending on the desired level of detail. The most common fire model, known as a *zone model*, generally uses two control volumes to describe a compartment – an upper layer and a lower layer. In the compartment with the fire, additional control volumes for the fire plume or the ceiling jet may be included to improve the accuracy of the prediction (see Figure 1). Additional zones can be added as necessity arises to cover extensions.

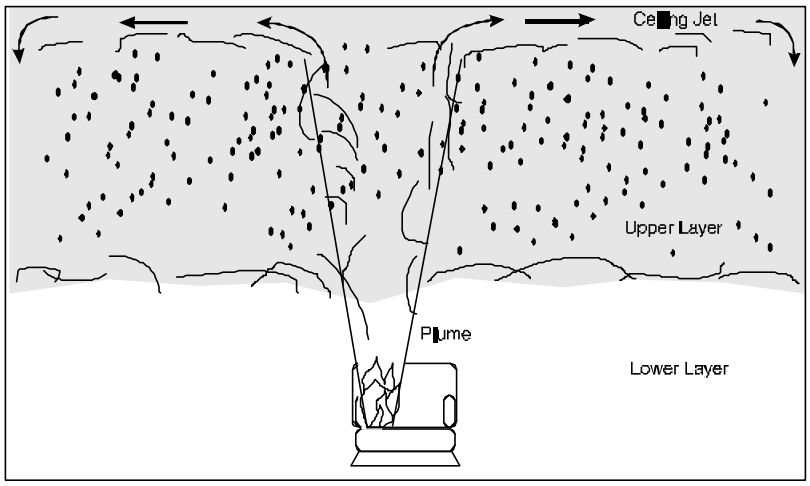

Figure 1. Zone model terms.

This two-layer approach has evolved from observation of such layering in real-scale fire experiments. Hot gases collect at the ceiling and fill the compartment from the top. While these experiments show some variation in conditions within the layer, these are small compared to the differences between the layers. Thus, the zone model can produce a fairly realistic simulation under most conditions.

Other types of models include *network models* and *field models*. Network models use one control volume per compartment and are used to predict conditions in spaces far removed from the fire compartment where temperatures are near ambient and layering does not occur. The field model

goes to the other extreme, dividing the compartment into thousands or even a million or more control volumes. Such models can predict the variation in conditions within the layers, but typically require far longer run times than zone models. Thus, they are used when highly detailed calculations are essential. We will use CFAST as an example for discussing the underlying physics of zone models, since it contains all of the phenomena which must be included. A list of similar models will be given at the end of the paper.

The modeling equations used in CFAST take the mathematical form of an initial value problem for a system of ordinary differential equations (ODE). These equations are derived using the conservation of mass, the conservation of energy (equivalently the first law of thermodynamics), the ideal gas law and relations for density and internal energy. These equations predict as functions of time quantities such as pressure, layer heights and temperatures given the accumulation of mass and enthalpy in the two layers. The CFAST model then consists of a set of ODEs to compute the environment in each compartment and a collection of algorithms to compute the mass and enthalpy source terms required by the ODEs.

Fires

A fire is as a source of fuel which is released at a specified rate. This fuel is converted into enthalpy (the conversion factor is the heat of combustion) and mass (the conversion factor is the yield of a particular species) as it burns. A fire is constrained if the enthalpy conversion depends on the oxygen concentration otherwise it is unconstrained. Burning can take place in the portion of the plume in the lower layer (if any), in the upper layer, or in a door jet. For an unconstrained fire, the burning will all take place within the fire plume. For a constrained fire, burning will take place where there is sufficient oxygen. When insufficient oxygen is entrained into the fire plume, unburned fuel will successively move into and burn in: the upper layer of the fire compartment, the plume in the doorway to the next compartment, the upper layer of the next compartment, the plume in the doorway to the third compartment, and so forth until it is consumed or gets to the outside.

Most models include the ability to track, independently, multiple fires in one or more compartments of the building. These fires are treated as totally separate entities, i.e., with no interaction of the plumes or radiative exchange between fires in a compartment. These fires are generally referred to as “objects” and can be ignited at a specified time, temperature or heat flux.

Plumes and Layers

A plume is formed above any burning object. It acts as a pump transferring mass and enthalpy from the lower layer into the upper layer. A correlation is used to predict the amount of mass and enthalpy that is transferred. A more complete plume model would predict plume entrainment by creating a separate zone and solving the appropriate equations.

Two sources exist for moving enthalpy and mass between the layers within and between compartments. Within the compartment, the fire plume provides one source. The other source of mixing between the layers occurs at vents such as doors or windows. Here, there is mixing at the boundary of the opposing flows moving into and out of the compartment. The degree of mixing is based on an empirically-derived mixing relation. Both the outflow and inflow entrain air from the

surrounding layers. The flow at vents is also modeled as a plume (called the door plume or jet), and uses the same equations as the fire plume, with two differences. First, an offset is calculated to account for entrainment within the doorway and second, the equations are modified to account for the rectangular geometry of vents compared to the round geometry of fire plumes. All plumes within the simulation entrain air from their surroundings according to an empirically-derived entrainment relation. Entrainment of relatively cool, non-smoke laden air adds oxygen to the plume and allows burning of the fuel. It also causes it to expand as the plume moves upward in the shape of an inverted cone. The entrainment in a vent is caused by bi-directional flow and results from vortices formed near a shear layer. This phenomenon called the Kelvin-Helmholtz instability. It is not exactly the same as a normal plume, so some error arises when this entrainment is approximated by a normal plume entrainment algorithm.

While experiments show that there is very little mixing between the layers at their interface, sources of convection such as radiators or diffusers of heating and air conditioning systems, and the downward flows of gases caused by cooling at walls, will cause such mixing. These are examples of phenomena which are not included because the theories are still under development. Also, the plumes are *assumed* not to be affected by other flows which may occur. For example, if the burning object is near the door the strong inflow of air will cause the plume axis to lean away from the door and affect entrainment of gases into the plume. Such effects are not included in the model.

As enthalpy and mass are pumped into the upper layer by the fire plume, the upper layer expands in volume causing the lower layer to decrease in volume and the interface to move downward. If the door to the next compartment has a soffit, there can be no flow through the vent from the upper layer until the interface reaches the bottom of that soffit. Thus in the early stages the expanding upper layer will push down on the lower layer air and force it into the next compartment through the vent by expansion.

Once the interface reaches the soffit level, a door plume forms and flow from the fire compartment to the next compartment is initiated. As smoke flow from the fire compartment fills the second compartment, the lower layer of air in the second compartment is pushed down. As a result, some of this air flows into the fire compartment through the lower part of the connecting doorway (or vent). Thus, a vent between the fire compartment and connecting compartments can have simultaneous, opposing flows of air. All flows are driven by pressure and density differences that result from temperature differences and layer depths. Thus the key to getting the right flows is to correctly distribute the fire and plume's mass and enthalpy between the layers.

Vent Flow

Flow through vents is a dominant component of any fire model because it is sensitive to small changes in pressure and transfers the greatest amount of enthalpy on an instantaneous basis of all the source terms (except of course for the fire and plume). Its sensitivity to environmental changes arises through its dependence on the pressure difference between compartments which can change rapidly. In the realm of zone modeling there are two distinct types of flow: horizontal flow through vertical vents (ceiling holes, hatches *etc.*) and vertical flow through horizontal vents (doors, windows *etc.*). Horizontal flow is the flow which is normally thought of when discussing

fires. Vertical flow is particularly important in two disparate situations: a ship, and the role of fire fighters doing roof venting.

Horizontal vent flow is determined using the pressure difference across a vent. Flow at a given elevation may be computed using Bernoulli's law by first computing the pressure difference at that elevation. The pressure on each side of the vent is computed using the pressure at the floor, the height of the floor and the density.

Atmospheric pressure is about 100 000 Pa, fires produce pressure changes from 1 Pa to 1000 Pa and mechanical ventilation systems typically involve pressure differentials of about 1 Pa to 100 Pa. The pressure variables are solved to a higher accuracy than other solution variables because of the subtraction (with resulting loss of precision) needed to calculate vent flows from pressure differences.

Heat Transfer

Gas layers exchange energy with their surroundings via convective and radiative heat transfer. While different material properties can be used for the ceiling, floor, and walls of each compartment, usually, material thermophysical properties are *assumed* to be constant, although we know that they vary somewhat with temperature. This assumption is made because data over the required temperature range is scarce even for common materials.

Radiative transfer occurs among the fire(s), gas layers and compartment surfaces (ceiling, walls and floor). This transfer is a function of the temperature differences and the emissivity of the gas layers as well as the compartment surfaces. For the fire and typical surfaces, emissivity values only vary over a small range. For the gas layers, however, the emissivity is a function of the concentration of species which are strong radiators: predominately smoke particulates, carbon dioxide, and water. Thus errors in the species concentrations can give rise to errors in the distribution of enthalpy among the layers, which results in errors in temperatures, resulting in errors in the flows.

Species Concentration and Deposition

When the layers are initialized at the start of the simulation, they are set to ambient conditions. These are the initial temperatures specified by the user, and 23 % by mass (20.8 % by volume) oxygen, 77 % by mass (79 % by volume) nitrogen, a mass concentration of water specified by the user as a relative humidity, and a zero concentration of all other species. As fuel is pyrolyzed, the various species are produced in direct relation to the mass of fuel burned (this relation is the species yield specified by the user for the fuel burning). Since oxygen is consumed rather than produced by the burning, the "yield" of oxygen is negative, and is set internally to correspond to the amount of oxygen needed to burn the fuel. Also, hydrogen cyanide and hydrogen chloride are assumed to be products of pyrolysis whereas carbon dioxide, carbon monoxide, water, and soot are products of combustion.

Each unit mass of a species produced is carried in the flow to the various compartments and accumulates in the layers. The model keeps track of the mass of each species in each layer, and

knows the volume of each layer as a function of time. The mass divided by the volume is the mass concentration, which along with the molecular weight gives the concentration in volume % or parts per million as appropriate.

No model of fire growth and smoke transport incorporates a complete combustion scheme. It is simply not practical at this time. Rather than try to capture the development of all species, it has been deemed more practical to use empirical methods: measure the rate of production of species and use these in the predictive model. For fires, a combustion chemistry scheme based on a carbon-hydrogen-oxygen balance is commonly used. The scheme needs to be applied in at least three places. The first is burning in the portion of the plume which is in the lower layer of the compartment of fire origin. The second is the portion in the upper layer, also in the compartment of origin. The third is in the vent flow which entrains air from a lower layer into an upper layer in an adjacent compartment. This is equivalent to solving the conservation equations for each species independently.

There are two significant limitations of zone models inherent in this prescription: it is difficult to capture the effect of transitioning through the layer interface, which is the one of the sources of carbon monoxide. The other is the transient nature of plume, especially in the initial phase of a fire when the plume is developing from a small cloud to a complete plume envisioned by Morten, Taylor and Turner in their classic tretise on plumes.

Predictive Equations

This section presents a derivation of the predictive equations for zone fire models[6], [8]. Zone fire models solve a set of equations in the form of an initial value problem for a mixed system of differential and algebraic equations. These equations are derived from the conservation of mass and energy. Subsidiary equations are the ideal gas law and definitions of density and internal energy (for example, see [11]). These conservation laws are invoked for each zone or control volume. For further information on the numerical implications of these choices please see reference [12].

The basic element of the model is a zone. The basic assumption of a zone model is that properties such as temperature can be approximated throughout the zone by some uniform function. The usual approximation is that temperature, density and so on are uniform within a zone. The assumption of uniform properties is reasonable and yields good agreement with experiment. In general, these zones are grouped within compartments.

There are two reasonable conjectures which dramatically improve the ease of solving these equations. Momentum is ignored within a compartment. The momentum of the interface has no significance in the present context. However, at boundaries such as windows, doors and so on, the Euler equation is integrated explicitly to yield the Bernoulli equation. This is solved implicitly in the equations which are discussed below. The other approximation is that the pressure is approximately uniform within a compartment. The argument is that a change in pressure of a few tens of Pascals over the height of the compartment is negligible in comparison with atmospheric pressure. Once again, this is applied to the basic conservation equations. This is consistent with the point source view of finite element models. Volume is merely one of the dependent variables.

However, the hydrostatic variation in pressure *is* taken into account in calculating pressure differences between compartments.

Many formulations based upon these assumptions can be derived. Several of these are discussed later. One formulation can be converted into another using the definitions of density, internal energy and the ideal gas law. Though equivalent analytically, these formulations differ in their numerical properties. Also, until the development of FAST [6], all models of this type assumed that the pressure equilibrated instantaneously, and thus the *dP/dt* term could be set to zero. However, as has been shown [13], it is better to solve these equations in the differential rather than the algebraic form if the proper solver is used.

As discussed in references [12] and [14], the zone fire modeling differential equations (ODE's) are stiff. The term stiff means that multiple time scales are present in the ODE solution. In our problem, pressures adjust to changing conditions much quicker than other quantities such as layer temperatures or interface heights. Special solvers are required in general to solve zone fire modeling ODE's because of this stiffness. Runge-Kutta methods or predictor-corrector methods such as Adams-Bashforth require prohibitively small time steps in order to track the short-time scale phenomena (pressure in our case). Methods that calculate the Jacobian (or at least approximate it) have a much larger stability region for stiff problems and are thus more successful at their solution.

Each formulation can be expressed in terms of mass and enthalpy flow. These rates represent the exchange of mass and enthalpy between zones due to physical phenomena such as plumes, natural and forced ventilation, convective and radiative heat transfer, and so on. For example, a vent exchanges mass and enthalpy between zones in connected rooms, a fire plume typically adds heat to the upper layer and transfers entrained mass and enthalpy from the lower to the upper layer, and convection transfers enthalpy from the gas layers to the surrounding walls.

We use the formalism that the mass flow to the upper and lower layers is denoted $\dot{m}_U$ and $\dot{m}_L$ and the enthalpy flow to the upper and lower layers is denoted $\dot{H}_U$ and $\dot{H}_L$. It is tacitly assumed that these rates may be computed in terms of zone properties such as temperature and density. These rates represent the net sum of all possible sources of mass and enthalpy due to phenomena such as those listed above. The numerical characteristics of the various formulations are easier to identify if the underlying physical phenomena are decoupled in this way.

Many approximations are necessary when developing physical sub-models for the mass and enthalpy terms. For example, most fire models assume that 1) the specific heat terms c_p and c_v are constant even though they depend upon temperature, 2) hydrostatic terms can be ignored in the equation of state (the ideal gas law) relating density of a layer with its temperature. However, the derivations which follow are all based on the basic conservation laws.

Derivation of Equations for a Two-Layer Model

A compartment is divided into two control volumes, a relatively hot upper layer and a relatively cooler lower layer, as illustrated in Figure 2. The gas in each layer has attributes of mass, internal energy, density, temperature, and volume denoted respectively by m_i, E_i, ρ_i, T_i, and V_i where $i=L$

for the lower layer and $i=U$ for the upper layer. The compartment as a whole has the attribute of pressure P. These 11 variables are related by means of the following seven constraints

$$\rho_i = \frac{m_i}{V_i} \quad \textbf{(density)} \tag{1}$$

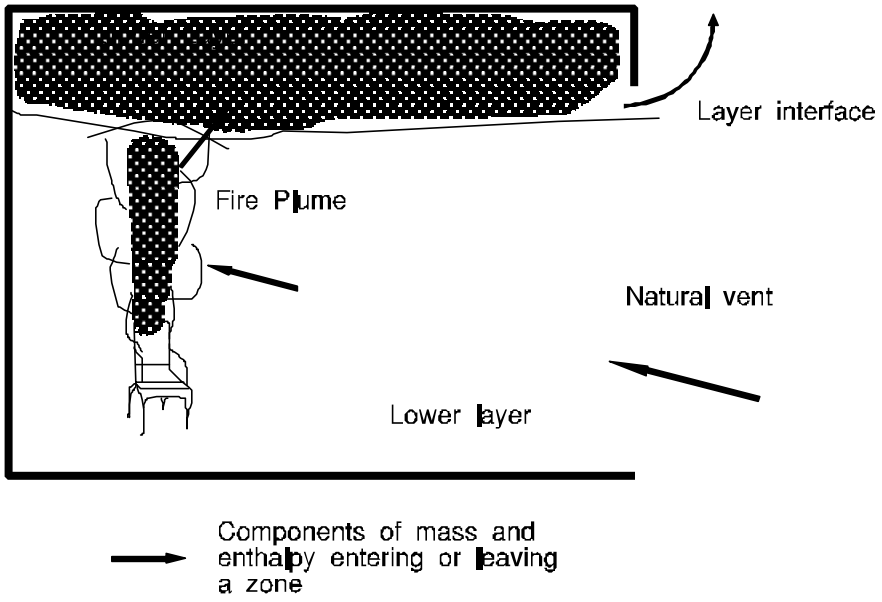

Figure 2. Schematic of control volumes in a two-layer zone model.

$$E_i = c_v m_i T_i \quad \textbf{(internal energy)} \tag{2}$$

$$P = R\rho_i T_i \quad \textbf{(ideal gas law)} \tag{3}$$

$$V = V_L + V_U \quad \textbf{(total volume)} \tag{4}$$

We get seven by counting density, internal energy and the ideal gas law twice (once for each layer). The specific heat at constant volume and at constant pressure c_v and c_p, the universal gas constant, R, and the ratio of specific heats, γ, are related by $\gamma = c_p / c_v$ and $R = c_p - c_v$. For air, c_p . 1000 kJ/kg K and $\gamma = 1.4$. Four additional equations obtained from conservation of mass and energy for each layer are required to complete the equation set. The differential equations for mass in each layer are

$$\begin{aligned} \frac{dm_L}{dt} &= \dot{m}_L \\ \frac{dm_U}{dt} &= \dot{m}_U \end{aligned} \tag{5}$$

The first law of thermodynamics states that the rate of increase of internal energy plus the rate at which the layer does work by expansion is equal to the rate at which enthalpy is added to the gas. In differential form this is

$$\underbrace{\frac{dE_i}{dt}}_{\text{internal energy}} + \underbrace{P\frac{dV_i}{dt}}_{\text{work}} = \underbrace{\dot{s}_i}_{\text{enthalpy}} \tag{6}$$

where c_v is taken as constant. A differential equation for pressure can be derived by adding the upper and lower layer versions of eq (6), noting that $dV_U/dt = -dV_L/dt$, and substituting the differential form of eq (2) to yield

$$\frac{dP}{dt} = \frac{\gamma - 1}{V}\left(\dot{s}_L + \dot{s}_U\right). \tag{7}$$

Differential equations for the layer volumes can be obtained by substituting the differential form of eq (2) into eq (6) to obtain

$$\frac{dV_i}{dt} = \frac{1}{P\gamma}\left((\gamma - 1)\,\dot{s}_i - V_i\frac{dP}{dt}\right). \tag{8}$$

Equation (6) can be rewritten using eq (8) to eliminate dV/dt to obtain

$$\frac{dE_i}{dt} = \frac{1}{\gamma}\left(\dot{s}_i + V_i\frac{dP}{dt}\right). \tag{9}$$

A differential equation for density can be derived by applying the quotient rule to $\frac{d\rho_i}{dt} = \frac{d}{dt}\left(\frac{m_i}{V_i}\right)$ and using eq (8) to eliminate dV_i/dt to obtain

$$\frac{d\rho_i}{dt} = -\frac{1}{c_p T_i V_i}\left(\left(\dot{s}_i - c_p\dot{m}_i T_i\right) - \frac{V_i}{\gamma - 1}\frac{dP}{dt}\right). \tag{10}$$

Temperature differential equations can be obtained from the equation of state by applying the quotient rule to $\frac{dT_i}{dt} = \frac{d}{dt}\left(\frac{P}{R\rho_i}\right)$ and using eq (10) to eliminate dD/dt to obtain

$$\frac{dT_i}{dt} = \frac{1}{c_p \rho_i V_i}\left(\left(\dot{s}_i - c_p \dot{m}_i T_i \right) + V_i \frac{dP}{dt} \right) . \qquad (11)$$

The time evolution of these solution variables can be computed by solving the corresponding differential equations together with appropriate initial conditions. The remaining seven variables can be determined from the four solution variables using eqs (1) to (4).

There are, however, many possible differential equation formulations. Indeed, there are 330 different ways to select four variables from eleven. Many of these systems are incomplete due to the relationships that exist between the variables given in eqs (1) to (4). For example the variables, D_U, V_U, m_U, and P form a dependent set since $D_U = m_U / V_U$.

The number of differential equation formulations can be considerably reduced by not mixing variable types between layers; that is, if upper layer mass is chosen as a solution variable, then lower layer mass must also be chosen. For example, for two of the solution variables choose m_L and m_U, or D_L and D_U, or T_L and T_U. For the other two solution variables pick E_L and E_U or P and V_L or P and V_U. This reduces the number of distinct formulations to nine. Since the numerical properties of the upper layer volume equation are the same as a lower layer one, the number of distinct formulations can be reduced to six.

Table 1. Conservative zone model equations

Equation Type	Differential Equation
i'th layer mass	$\frac{dm_i}{dt} = \dot{m}_i$
pressure	$\frac{dP}{dt} = \frac{\gamma - 1}{V}\left(\dot{s}_L + \dot{s}_U \right)$
i'th layer energy	$\frac{dE_i}{dt} = \frac{1}{\gamma}\left(\dot{s}_i + V_i \frac{dP}{dt} \right)$
i'th layer volume	$\frac{dV_i}{dt} = \frac{1}{\gamma P}\left((\gamma - 1)\dot{s}_i - V_i \frac{dP}{dt} \right)$
i'th layer density	$\frac{d\rho_i}{dt} = -\frac{1}{c_p T_i V_i}\left(\left(\dot{s}_i - c_p \dot{m}_i T_i \right) - \frac{V_i}{\gamma - 1}\frac{dP}{dt} \right)$
i'th layer temperature	$\frac{dT_i}{dt} = \frac{1}{c_p \rho_i V_i}\left(\left(\dot{s}_i - c_p \dot{m}_i T_i \right) + V_i \frac{dP}{dt} \right)$

An Example Implementation

At this point, incorporating phenomena is a matter of providing an algorithm which calculate the mass and enthalpy flux. These terms are then added to the right-hand side of the above equations ($\dot{s}$ for energy and $\dot{m}$ for mass). The following are some detailed examples of how these terms can be treated. These is not an exhaustive tretise, but covers some of the more difficult issues.

Specified Fire

A specified fire is one for which the time dependent characteristics are specified as a function of time. The specified fire can be unconstrained (type 1) or constrained (type 2). The heat release rate for a constrained fire may be reduced below its specified value based upon the concentration of fuel or oxygen available for combustion. Combustion chemistry is not calculated for type 1 fires. The pyrolysis rate for both fire types is specified as $\dot{m}_f$, the burning rate as $\dot{m}_b$ and the heat of combustion as H_c so that the heat release rate, $\dot{Q}_f$, is

$$\dot{Q}_f = H_c \dot{m}_b - c_p \left(T_u - T_0\right) \dot{m}_b \tag{12}$$

For an unconstrained fire, $\dot{m}_b = \dot{m}_f$, whereas for the constrained fire, $\dot{m}_b < \dot{m}_f$, or equivalently the burning rate may be less than the pyrolysis rate. Models of specified fires generally use an effective heat of combustion which is obtained from an experimental apparatus such as the cone calorimeter [15]. A shortcoming of this approach is that it does not account for increased pyrolysis due to radiative feedback from the flame or compartment. In an actual fire, this is an important consideration, and the specification used should match the experimental conditions as closely as possible.

The enthalpy which is released goes into radiation and convection

$$\begin{aligned} \dot{Q}_r(fire) &= \chi_R \dot{Q}_f \\ \dot{Q}_c(fire) &= \left(1 - \chi_R\right) \dot{Q}_f . \end{aligned} \tag{13}$$

where, χ_R , is the fraction of the fire's heat release rate given off as radiation. The convective heat release rate, $\dot{Q}_c(fire)$ then becomes the driving term in the plume flow. For a specified fire there is radiation to both the upper and lower layers, whereas the convective part contributes only to the upper layer.

Combustion Chemistry

The second type of fire is constrained by the amount of available oxygen. The latter scheme is applied in three places. The first is burning in the portion of the plume which is in the lower layer of the room of fire origin (region #1). The second is the portion of the plume in the upper layer, also in the room of origin (region #2). The third is in the vent flow which entrains air from a lower layer into an upper layer in an adjacent compartment (region #3).These are shown schematically in Figure 3.

The species which are affected by this scheme are O_2, CO_2, CO, H_2O, unburned hydrocarbons (TUHC), and soot (OD). Nitrogen is carried as a gas, but only acts as a diluent. There are at present no nitrogen reactions. In a chemical equation, the individual atoms on the left and right hand sides must balance. This is true regardless of whether the reaction is considered to be stoichiometric (complete). We apply this idea to the combination of fuel and oxygen to yield a balance of number density (#/volume). In terms of the "regions," (Figure 3), we have

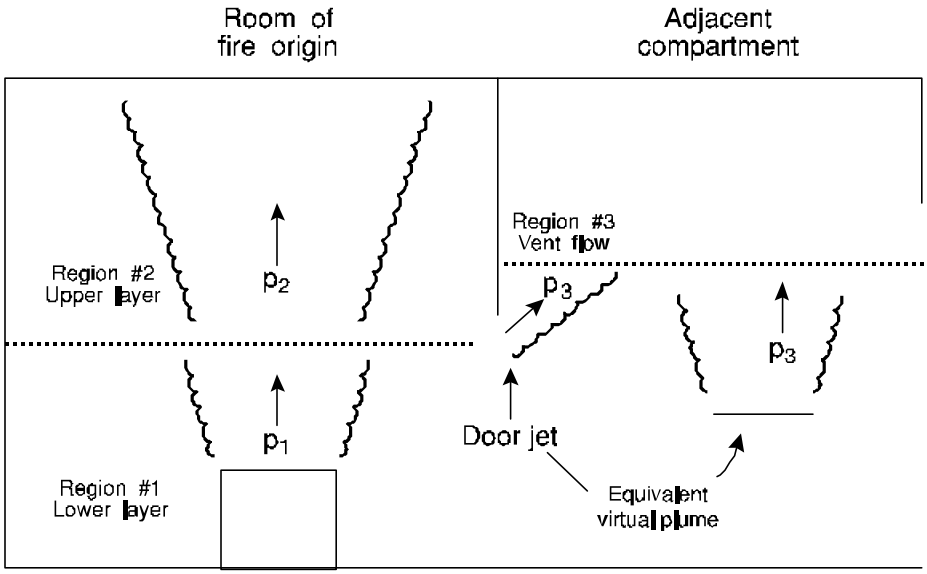

Figure 3. Schematic of entrainment and burning regions.

$\dot{m}_f$ = pyrolysis rate of the source (kg/sec) (region #1)

or

$\dot{m}_f = \dot{m}_{tuhc}$ from a previous region (kg/sec) (region #2 and #3).

and

$$\dot{m}_{tuhc} = \dot{m}_f - \dot{m}_b$$

where *tuhc* stands for total un-burned hydrocarbons.

The simplest form of energy release is made by specifying a heat release rate, together with a consistent mass release rate. This would simulate the fire that occurs in an unconfined space. As soon as one is constrained by the confines of a compartment, then the nature of the fire changes. In particular the available oxygen may not be sufficient to allow complete combustion. However, it is not consistent to try to account for the oxygen alone. All pertinent species must be followed.

The essence of the species production scheme which we now utilize is to allow as realistic fuel composition as possible, i.e., include oxygen, carbon, hydrogen and chlorine as part of the fuel. Carbon monoxide, carbon dioxide, soot, water, hydrogen cyanide and hydrogen chloride are the products of combustion. The fuel properties are specified as H/C, HCl/C, HCN/C and O/C which are mass ratios of hydrogen, hydrochloric acid, hydrogen cyanide and oxygen to carbon respectively. The production properties are HCl/f, HCN/f, CO/CO_2, and S/CO_2 which again are mass ratios. The chemical symbols used here have their usual meaning, except for soot. The subscript "S" is used to designate soot, and we assume it consists primarily of carbon, at least by mass.

The fuel burning rate in terms of the carbon production is

$$\dot{m}_f = \{-\} \times \dot{m}_c \tag{14}$$

where {—} is the multiplier in the fuel production defined as

$$\{-\} = \left(1 + \frac{H}{C} + \frac{HCl}{C} + \frac{HCN}{C} + \frac{O}{C}\right) = f/C. \tag{15}$$

In order to avoid detailed chemical kinetics, it is common to use the oxygen consumption concept [16], [17] to relate the mass loss to the heat release rate. The following derivation is for the heat release rate as a function of the fuel burning rate, and the heat release rate based on oxygen consumption. H/C, HCl/C, HCN/C and O/C are the ratio of mass of that species to carbon in the fuel. Thus H/C is for the mass of hydrogen to the mass of carbon produced in pyrolysis. This is a very useful way to characterize the fuel. This is in terms of the elemental composition of the fuel, and not elemental molecules, such as H_2. These are the ratios for the fuel, and the material which comes from it. For the products of the combustion process, we have CO_2/C, CO/C, H_2O/C and S/C. These ratios are in terms of free molecules, generally gaseous.

The first step is to limit the actual burning which takes place in the combustion zone. In each combustion zone, there is a quantity of fuel available. At the source this results from the pyrolysis of the material, m_f. In other situations such as a plume or door jet, it is the net unburned fuel available, m_{TUHC}. In each case, the fuel which is available but not burned is then deposited into the "m_{TUHC}" category. This provides a consistent notation. In the discussion below, m_f is the amount of fuel burned. This value is initialized to the available fuel, and then reduced if there is insufficient oxygen to support complete combustion. Subsequently, the available fuel, m_{TUHC}, is reduced by the final value of m_f. Thus we have a consistent description in each burning region, with an algorithm that can be invoked independent of the region being analyzed.

$$\dot{Q} = \dot{m}_f \times H_c \ , \tag{16}$$

with the mass of oxygen required to achieve this energy release rate (based on the oxygen consumption principle [18]) of

$$\dot{m}_O = \frac{\dot{Q}}{1.32\times10^7} = \dot{m}_f \times \frac{H_c}{1.32\times10^7} \,. \tag{17}$$

If the fuel contains oxygen (available for combustion), the oxygen needed to achieve full combustion is less than this value

$$\dot{m}_O(\text{needed}) = \dot{m}_O - \dot{m}_O(\text{in the fuel}) \tag{18}$$

If sufficient oxygen is available, then it is fully burned. However, if the oxygen concentration is low enough, it will constrain the burning and impose a limit on the amount of fuel actually burned, as opposed to the amount pyrolyzed. The actual limitation is discussed below and is presented as eq (21).

$$\dot{m}_O(\text{actual}) = \text{minimum of} \left\{ \dot{m}_O(\text{available}), \dot{m}_O(\text{needed}) \right\}, \tag{19}$$

$$\dot{m}_f(\text{actual}) = \dot{m}_O(\text{actual}) \times \frac{1.32\,x\,10^7}{H_c} \tag{20}$$

Essentially, we limit the amount of fuel that is burned, as opposed to the amount that is pyrolyzed, to the lesser of the amount pyrolyzed and that required to consume the *available* oxygen. The $\dot{m}_O$(actual) and $\dot{m}_f$(actual) are the quantities used below. By way of explanation, eq (16) tells us how much energy would be released by the available fuel if there were no constraint (free burn). Equation (17) then tells us the mass of oxygen required to achieve this energy release rate. The relationship is based on the work in reference [19]. Equation (18) yields the amount needed based on the required amount less the oxygen available in the fuel. Solid propellant would yield a value of zero at this point. Equation (19) limits the amount used and eq (20) then yields the amount of fuel actually burned, as opposed to the amount pyrolyzed.

The form in which we cast these equations evolves naturally from the properties of combustion. Hydrogen, carbon and bound oxygen are properties of the fuel. They can be measured experimentally independent of the combustion process. Thus we use these ratios as the basis of the scheme. In a similar sense, hydrogen chloride and hydrogen cyanide are properties of the pyrolysis process. So hydrogen chloride and hydrogen cyanide production are specified with respect to the fuel pyrolysis. Normally this is how they are measured, for example with the cone calorimeter, so we can use the measured quantities directly. Other than the cyanide, chloride and water production, hydrogen does not play a role. In general, hydrogen has a much greater affinity for oxygen than carbon, so almost all of the hydrogen will be utilized. This dictates our next choice, which is that soot is essentially all carbon. On a mass basis, this is certainly true. On a molecular basis, however, it may not be so simple. Carbon dioxide is a direct product of combustion, and the assumption is that most carbon will end up here. Carbon monoxide and soot are functions of incomplete combustion. Thus they depend on the environment in which the burning takes place. They are in no case a function of the pyrolysis process itself. Thus the production of these products is specified with respect to the carbon dioxide. At present, we must rely on measured ratios, but this is beginning to change as we gain a better understanding of the

combustion process. So, in the present model, carbon goes to one of three final species, carbon dioxide, carbon monoxide or soot, with the particular branching ratio depending on the chemistry active at the time.

The relationship between oxygen and fuel concentration defines a range where burning will take place. The rich limit is where, for a given ratio of O_2 to N_2 (generally the ratio in air), there is too much fuel for combustion. At the other end, there is the lean flammability limit, where there is too little fuel for combustion. Often the rich limit is incorporated by limiting the burning rate as the oxygen level decreases until a “lower oxygen limit” (LOL) is reached. The lower oxygen limit is incorporated through a smooth decrease in the burning rate near the limit:

$$\dot{m}_o(available) = \dot{m}_e Y_{O_2} C_{LOL} \tag{21}$$

where m_e is the mass entrainment flow rate and the lower oxygen limit coefficient, C_{LOL}, is the fraction of the available fuel which can be burned with the available oxygen and varies from 0 at the limit to 1 above the limit. An example of a functional form which provides a smooth cutoff of the burning over a narrow range above the limit is

$$C_{LOL} = \frac{\tanh\left(800\left(Y_{O_2} - Y_{LOL}\right) - 4\right) + 1}{2} \tag{22}$$

For the lean flammability limit, an ignition temperature criterion is included, below which no burning takes place.

As stated, the burning rate simply decreases as the oxygen level decreases. We know that there is an oxygen concentration below which fuel will not oxidize. This is referred to as the "rich flammability" limit. In the present context we refer to this point as the lower oxygen limit (LOL). At the other end, there is a "lean flammability" limit. The fuel oxidation rate is limited at both ends. At present, we have incorporated only the rich flammability limit. We do not have sufficient theoretical underpinnings, nor sufficient experimental data, to include temperature dependence of the lean flammability limit. In the lean flammability limit, we use only a temperature criterion below which we assume no burning takes place.

In summary, we can predict the formation of some of the products of combustion, carbon dioxide, carbon monoxide, soot, water, hydrogen cyanide, and hydrogen chloride given the branching ratios CO/CO_2, $S(soot)/CO_2$, the composition of the fuel, H/C, O/C, HCl/f and HCN/f and the flammability limit. At present, in practice we use experimental values, such as those from Morehart *et al.*[20]. The composition of the fuel is a measurable quantity, although it is complicated somewhat by physical effects. The complication arises in that materials such as wood will yield methane in the early stages of burning, and carbon rich products at later times. Thus the H/C and O/C ratios are functions of time. Finally, the production ratios of CO/CO_2, $S(soot)/CO_2$ are based on the kinetics which in turn is a function of the ambient environment.

Vent Flow

Mass flow (in the remainder of this section, the term “flow” will be used to mean mass flow) is the dominant source term for the predictive equations because it fluctuates most rapidly and transfers the greatest amount of enthalpy on an instantaneous basis of all the source terms (except of course the fire). Also, it is most sensitive to changes in the environment. CFAST models horizontal flow through vertical vents and vertical flow through horizontal vents. Horizontal flow encompasses flow through doors, windows and so on. Vertical flow occurs in ceiling vents. It is important in two separate situations: on a ship with open hatches and in house fires with roof venting.

Horizontal Flow Through Vertical Vents

Flow through normal vents such as windows and doors is governed by the pressure difference across a vent. A momentum equation for the zone boundaries is not solved directly. Instead momentum transfer at the zone boundaries is included by using an integrated form of Euler's equation, namely Bernoulli's solution for the velocity equation. This solution is augmented for restricted openings by using flow coefficients [21] to allow for constriction from finite size doors. The flow (or orifice) coefficient is an empirical term which addresses the problem of constriction of velocity streamlines at an orifice.

Bernoulli's equation is the integral of the Euler equation and applies to general initial and final velocities and pressures. The implication of using this equation for a zone model is that the initial velocity in the doorway is the quantity sought, and the final velocity in the target compartment vanishes. That is, the flow velocity vanishes where the final pressure is measured. Thus, the pressure at a stagnation point is used. This is consistent with the concept of uniform zones which are completely mixed and have no internal flow. The general form for the velocity of the mass flow is given by

$$v = C\left(\frac{2\Delta P}{\rho}\right)^{1/2} \tag{23}$$

where C is the constriction (or flow) coefficient ($.0.7$), D is the gas density on the source side, and $)P$ is the pressure across the interface. (Note: at present we use a constant C for all gas temperatures.)

The simplest means to define the limits of integration is with neutral planes, that is the height at which flow reversal occurs, and physical boundaries such as sills and soffits. By breaking the integral into intervals defined by flow reversal, a soffit, a sill, or a zone interface, the flow equation can be integrated piecewise analytically and then summed.

The approach to calculating the flow field is of some interest. The flow calculations are performed as follows. The vent opening is partitioned into at most six slabs where each slab is bounded by a layer height, neutral plane, or vent boundary such as a soffit or sill. The most general case is illustrated in Figure 4.

The mass flow for each slab can be determined from

$$\dot{m}_{1\to 2} = \frac{1}{3} C(\Delta\rho) A_{slab} \left(\frac{x^2 + xy + y^2}{x+y} \right) \tag{24}$$

where $x = |P_t|^{1/2}$, and $y = |P_b|^{1/2}$. P_t and P_b are the cross-vent pressure differential at the top and bottom of the slab respectively and A_{slab} is the cross-sectional area of the slab. The value of the density, D, is taken from the source compartment.

A mixing phenomenon occurs at vents which is similar to entrainment in plumes. As hot gases from one compartment leave that compartment and flow into an adjacent compartment a door jet can exist which is analogous to a normal plume.

The other type of mixing is much like an inverse plume and causes contamination of the lower layer. It occurs when there is flow of the type $\dot{m}_{42} > 0$. The shear flow causes vortex shedding into the lower layer and thus some of the particulates end up in the lower layer. The actual amount of mass or energy transferred is usually not large, but its effect can be large. For example, even minute amounts of carbon can change the radiative properties of the gas layer, from negligible to something finite. It changes the rate of radiation absorption by orders of magnitude and invalidates the simplification of an ambient temperature lower layer. This term is predicated on the Kelvin-Helmholz flow instability and requires shear flow between two separate fluids. The mixing is enhanced for greater density differences between the two layers. However, the amount of mixing has never been well characterized. Quintiere *et al*. discuss this phenomena for the case of crib fires in a single room, but their correlation does not yield good agreement with experimental data in the general case [22].

Vertical Flow Through Horizontal Vents

Flow through a ceiling or floor vent can be somewhat more complicated than through door or window vents. The simplest form is uni-directional flow, driven solely by a pressure difference. This is analogous to flow in the horizontal direction driven by a piston effect of expanding gases. Once again, it can be calculated based on the Bernoulli equation, and presents little difficulty. However, in general we must deal with more complex situations that must be modeled in order to have a proper understanding of smoke movement. The first is an occurrence of puffing. When a fire exists in a compartment in which there is only one hole in the ceiling, the fire will burn until the oxygen has been depleted, pushing gas out the hole. Eventually the fire will die down. At this point ambient air will rush back in, enable combustion to increase, and the process will be repeated. Combustion is thus tightly coupled to the flow. The other case is exchange flow which occurs when the fluid configuration across the vent is unstable (such as a hotter gas layer underneath a cooler gas layer). Both of these pressure regimes require a calculation of the onset of the flow reversal mechanism.

Normally a non-zero cross vent pressure difference tends to drive unidirectional flow from the higher to the lower pressure side. An unstable fluid density configuration occurs when the pressure alone would dictate stable stratification, but the fluid densities are reversed. That is, the hotter gas is underneath the cooler gas. Flow induced by such an unstable fluid density configuration tends to lead to bi-directional flow, with the fluid in the lower compartment rising into the upper compartment. This situation might arise in a real fire if the room of origin suddenly had a

hole punched in the ceiling. We make no pretense of being able to do this instability calculation analytically. We use Cooper's algorithm [23] for computing mass flow through ceiling and floor vents. It is based on correlations to model the unsteady component of the flow. What is surprising is that we can find a correlation at all for such a complex phenomenon. There are two components to the flow. The first is a net flow dictated by a pressure difference. The second is an exchange flow based on the relative densities of the gases. The overall flow is given by [23]

$$\dot{m} = C f(\gamma,\varepsilon) \left(\frac{\delta P}{\rho} \right)^{1/2} A_v \tag{25}$$

where $\gamma = c_p/c_v$ is the ratio of specific heats and

$$C = 0.68 + 0.17\varepsilon, \tag{26}$$

$$\varepsilon = \frac{\delta P}{P}, \tag{27}$$

and f is a weak function of both γ and ε. In the situation where we have an instability, we use Cooper's correlations. The algorithm for this exchange flow is given by

$$\dot{m}_{ex} = 0.1 \left(\frac{g\,\delta\rho\, A_v^{5/2}}{\rho_{av}} \right) \left(1.0 - \frac{2\,A_v^2\,\delta\rho}{S^2\,g\,\delta\rho\,D^5} \right) \tag{28}$$

where

$$D = 2\sqrt{\frac{A_v}{\pi}} \tag{29}$$

and S is 0.754 or 0.942 for round or square openings, respectively.

Forced Flow

Fan-duct systems are commonly used in buildings for heating, ventilation, air conditioning, pressurization, and exhaust. These systems are intended for applications where there is sufficient natural air leakage through cracks in walls and around windows and doors for odor control. Further information about these systems is presented in Klote and Milke [24] and the American Society of Heating, Refrigerating and Air Conditioning Engineers [25]. The model for mechanical ventilation used in CFAST is based on the theory of networks and is based on the model developed by Klote [26]. This is a simplified form of Kirchoff's law which says that flow into a node must be balanced by flow out of the node. Adapting Ohm's law,

$$\text{voltage} = \text{current} \times \text{resistance},$$

to HVAC flow, we have

pressure change = mass flow × resistance

which can then be written equivalently

mass flow = conductance × (pressure drop across a resistance)^{½} .

For each node, this flow must sum to zero. There are several assumptions which are made in computing this flow in ducts, fans, elbow, *etc*. The particular implementation used here [26] does not allow for reverse flow in the fans. The difficulty lies in describing how a fan behaves in such a case.

Given that we can describe mass flow in terms of pressure differences and conductance, the conservation equation for each node is

$$f_i(P_1, P_2, \ldots) = \sum_j \dot{m}_{ij} = 0. \tag{30}$$

The index "*j*" is a summation over connections to a node, and there is an equation "*i*" for each node. The remaining problem is to specify the boundary conditions. At each connection to a compartment, the pressure is specified. Then, given that flow at each connection is unidirectional (at a given instant of time, the flow is either all into or all out of a given connection), the mass and enthalpy flow into or out of a room can be calculated explicitly.
The equations describe the relationship between the pressure drop across a duct, the resistance of a duct, and the mass flow. The pressure can be changed by conditions in a compartment, or a fan in line in the duct system. Resistance arises from the finite size of ducts, roughness on surfaces, bends and joints. To carry the electrical analog a little further, fans act like constant voltage sources. The analogy breaks down in this case because the pressure (voltage) is proportional to the square of the velocity (current) rather than linearly related as in the electrical case. Since we are using the current form of the conservation equation to balance the system, the flow can be recast in terms of a conductance

$$\dot{m} = G\sqrt{\Delta P}. \tag{31}$$

The conductance can be expressed generally as

$$G = \sqrt{\frac{2\rho}{C_0}} A_0 \tag{32}$$

where C_0 is the flow coefficient, and A_0 is the area of the inlet, outlet, duct, contraction or expansion joint, coil, damper, bend, filter, and so on. Their values for the most common of these items are tabulated in the ASHRAE Handbook [27].

Ducts

Ducts are long pipes through which gases can flow. They have been studied much more extensively than other types of connections. For this reason, eq (32) can be put into a form which allows one to

characterize the conductance in more detail, depending on the type of duct (e.g., oval, round, or square) and is given by

$$G = \sqrt{\frac{FL}{2\rho D_e A_0^2}}, \tag{33}$$

where F is the friction factor, L and D_e are the length and effective diameter of the duct respectively. The temperature for each duct d is determined using the following differential equation:

accumulated heat = (heat in - heat out) - convective losses through duct walls

$$c_v \rho_d V_d \frac{dT_d}{dt} = c_p m_d (T_{in} - T_{out}) - h_d A_d (T_d - T_{amb}) \tag{34}$$

where c_v, c_p are the constant volume/pressure specific heats; V_d is the duct volume, D_d is the duct gas density, dT_d/dt is the time rate of change of the duct gas temperature, m_d is the mass flow rate, T_{in} and T_{out} are the gas temperatures going into and out of the duct, c_d, A_d are the convective heat transfer coefficient and surface area for duct d and T_{amb} is the ambient temperature. The first term on the right hand side of eq (34) represents the net gain of energy due to gas transported into or out of the duct. The second term represents heat transferred to the duct walls due to convection. In version 1.6, the loss coefficient is set to zero.

Fans

Normal fan operating range is represented by the line segment *AB* in Figure 8. In this figure, $)p_f$ is the static pressure of the fan, and $\dot{V}_f$ is the volumetric flow of the fan. The point *B* represents a margin of safety selected by the fan manufacturer in order to avoid unstable flow.

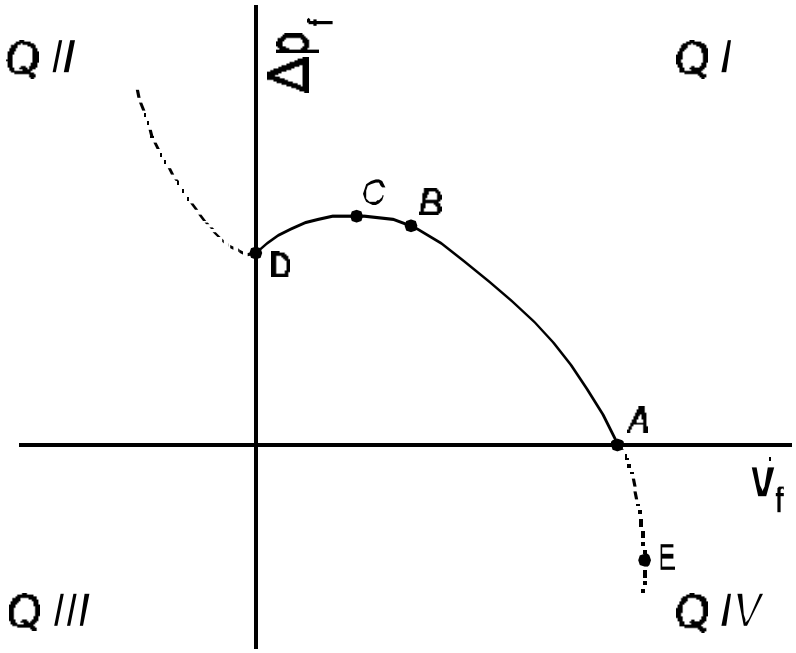

Figure 4. Typical fan performance at constant speed.

Fans operating in the positively sloping portion (*CD* of Figure 8) of the fan curve exhibit unstable behavior called surging or pulsing. Unstable flow consists of violent flow reversals accompanied by significant changes in pressure, power and noise. There is little information about how long a fan can operate in the unstable region before it is destroyed.

Backward flow through a fan occurs when the static pressure is greater than that at point *D*. This is also called second quadrant flow. Quadrant terminology is customarily used in description of fan performance. The horizontal axis and the vertical axis divide a plane into four quadrants which for convenience are labeled Q I, Q II, Q III and Q IV on Figure 8. Backward flow can be exhibited by all types of fans. The wind blowing into the outlet of a propeller fan can result in backflow, and pressures produced by fires could also produce backflow. Fourth quadrant flow is probably representative of all fans. As $)p_f$ becomes negative, the flow increases with decreasing $)p_f$ until a choking condition develops at point *E*.

Fan manufacturers generally supply flow-pressure data for the normal operating range, and they often supply data for the rest of the fan curve in the first quadrant. Specific data is not available for either second or fourth quadrant flow. No approach has been developed for simulation of unstable fan operation, and numerical modeling of unstable flow would be a complicated effort requiring research.

Corridor Flow

A standard assumption in zone fire modeling is that once hot smoke enters a compartment, a well defined upper layer forms instantly throughout the compartment. This assumption breaks down in large compartments and long corridors due to the time required to fill these spaces. A simple procedure is described for accounting for the formation delay of an upper layer in a long corridor by using correlations developed from numerical experiments generated with the NIST fire model FDS (Fire Dynamics Simulator) [28]. FDS is a computational fluid dynamics model capable of simulating fire flow velocities and temperatures with high resolution. Two parameters related to corridor flow are then estimated, the time required for a ceiling jet to travel in a corridor and the temperature distribution down the corridor. These estimates are then used in CFAST by delaying flow into compartments connected to corridors until the ceiling jet has passed these compartments. IFS was used to estimate ceiling jet characteristics by running a number of cases for various inlet layer depths and temperatures. A vent flow algorithm in then uses this information to compute mass and enthalpy flow between the corridor and adjacent compartments. This is accomplished by presenting the vent algorithm with a one layer environment (the lower layer) before the ceiling jet reaches the vent and a two layer environment afterwards. The zone fire model then uses these correlations to estimate conditions in the corridor.

Corridor Jet Flow Characteristics

Ceiling jet flow in a corridor can be characterized as a one dimensional gravity current. To a first approximation, the velocity of the current depends on the difference between the density of the gas located at the leading edge of the current and the gas in the adjacent ambient air. The velocity also depends on the depth of the current below the ceiling. A simple formula for the gravity current velocity may be derived by equating the potential energy of the current, $mgd_0/2$, measured at the half-height $d_0/2$ with its kinetic energy, $mU^2/2$ to obtain

$$U=\sqrt{gd_0}$$

where m is mass, g is the acceleration of gravity, d_0 is the height of the gravity current and U is the velocity. When the density difference, between the current and the ambient fluid is small, the velocity U is proportional to $\sqrt{gd_0\Delta\rho/\rho_{cj}}=\sqrt{gd_0\Delta T/T_{amb}}$ where ρ_{amb}, T_{amb} are the ambient density and temperature and ρ_{cj}, T_{cj} are the density and temperature of the ceiling jet and $\Delta T = T_{cj} - T_{amb}$ is the temperature difference. Here use has been made of the ideal gas law, $\rho_{amb}T_{amb} \approx \rho_{cj}T_{cj}$ This can be shown using terms defined in Figure 5 by using an integrated form of Bernoulli's law noting that the pressure drop at the bottom of the ceiling jet is $P_b = 0$, the pressure drop at the top is $P_t=gd_0(\rho_{cj}-\rho_{amb})$ and using a vent coefficient c_{vent} of 0.74, to obtain

$$
\begin{aligned}
U_0 &= c_{vent}\frac{\sqrt{8}}{3}\frac{1}{\sqrt{\rho_{cj}}}\frac{P_t+\sqrt{P_tP_b}+P_b}{\sqrt{P_t}+\sqrt{P_b}} \\
&= c_{vent}\frac{\sqrt{8}}{3}\sqrt{P_t/\rho_{cj}} \\
&= c_{vent}\frac{\sqrt{8}}{3}\sqrt{gd_0\frac{\rho_{amb}-\rho_{cj}}{\rho_{cj}}} \\
&\approx 0.7\sqrt{gd_0\frac{\Delta T}{T_{amb}}}
\end{aligned}
\tag{36}
$$

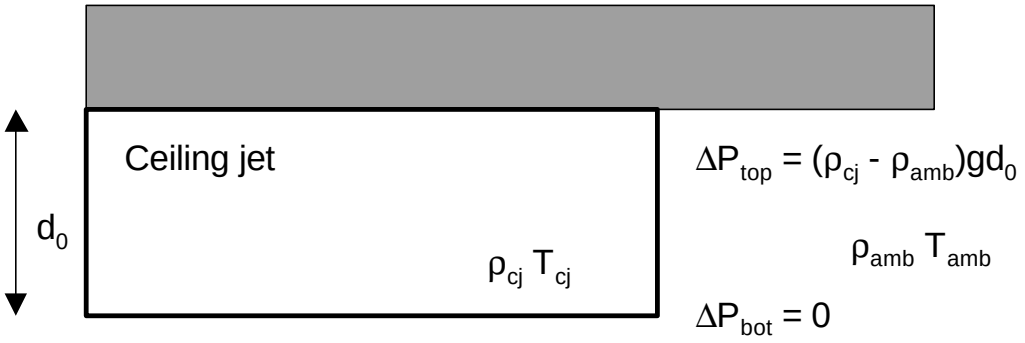

Figure 5 Schematic of a gravity current defining terms used to estimate its inlet velocity

Formulas of the form of the above equation lead one to conclude that a ceiling jet's characteristics in a corridor depend on its depth, d_0, and relative temperature difference, $\Delta T/T_{amb}$. Therefore, as the jet cools, it slows down. If no heat transfer occurs between the ceiling jet and the surrounding walls, then the only mechanism for cooling is mixing with surrounding cool air.

Heat Transfer

Radiation, convection and conduction are the primary mechanisms by which heat is transferred between the gas layers and the enclosing compartment walls. Convection, conduction and radiation are the nominal mechanisms for heat transfer and implementation of these are fairly uniform throughout the modeling community. Radiation can be somewhat tricky and is discussed in detail in this section.

Objects such as walls, gases and fires radiate as well as absorb radiation. Each object has its own properties, such as temperature and emissivity. As we are solving the enthalpy equation for the gas temperature, the primary focus is in finding out how much enthalpy is gained or lost by the gas layers due to radiation. To calculate the radiation absorbed in a zone, a heat balance must be done which includes all surfaces which radiate to and absorb radiation from a zone. The form of the terms which contribute heat to an absorbing layer are the same for all layers. Essentially we

assume that all zones in these models are similar so we can discuss them in terms of a general layer contribution. For this calculation to be done in a time commensurate with the other sources, some approximations are necessary.

Radiation can leave a layer by going to another layer, by going to the walls, by exiting through a vent, by heating an object, or by changing the pyrolysis rate of the fuel source. Similarly, a layer can be heated by absorption of radiation from these surfaces and objects as well as from the fire itself. The formalism which we employ for the geometry and view factor calculation is that of Siegel and Howell [30]. Although the radiation could be done with a great deal of generality, we have assumed that the zones and surfaces radiate and absorb like a grey body.

Radiation is an important mechanism for heat exchange in compartments subject to fires. It is important in the present application because it can affect the temperature distribution within a compartment, and thus the buoyancy forces. In the present implementation the fire is assumed to be a point source; it is assumed that plumes do not radiate. We use a simplified geometrical equivalent of the compartment in order to calculate the radiative transfer between the ceiling, floor and layer(s). A radiative heat transfer calculation could easily dominate the computation in any fire model. This is because radiation exchange is a global phenomena. Each portion of an enclosure interacts radiatively with every other portion that it “sees.” Therefore, it is important to construct algorithms for radiative heat transfer that are both accurate and efficient [29].

A common way to compute radiative heat exchange is based upon the equations developed in Siegel and Howell [30] which in turn is based on the work of Hottel [31]. Siegel and Howell model an enclosure with N wall segments and an interior gas. A radiation algorithm for a two layer zone fire model requires treatment of an enclosure with two uniform gases. Hottel and Cohen [32] developed a method where the enclosure is divided into a number of wall and gas volume elements. An energy balance is written for each element. Each balance includes interactions with all other elements. Treatment of the fire and the interaction of the fire and gas layers with the walls is based upon the work of Yamada and Cooper [33]. They model fires as point heat sources radiating uniformly in all directions and use the Lambert-Beer law to model the interaction between heat emitting elements (fires, walls, gas layers) and the gas layers. The original formulation is for an N-wall configuration. Although this approach would allow arbitrary specification of compartment surfaces (glass window walls, for example), the computational requirements are significant.

The radiation exchange at the k'th surface is shown schematically in Figure 6. For each wall segment k from 1 to N, we must find a net heat flux, $) q_k''$, such that

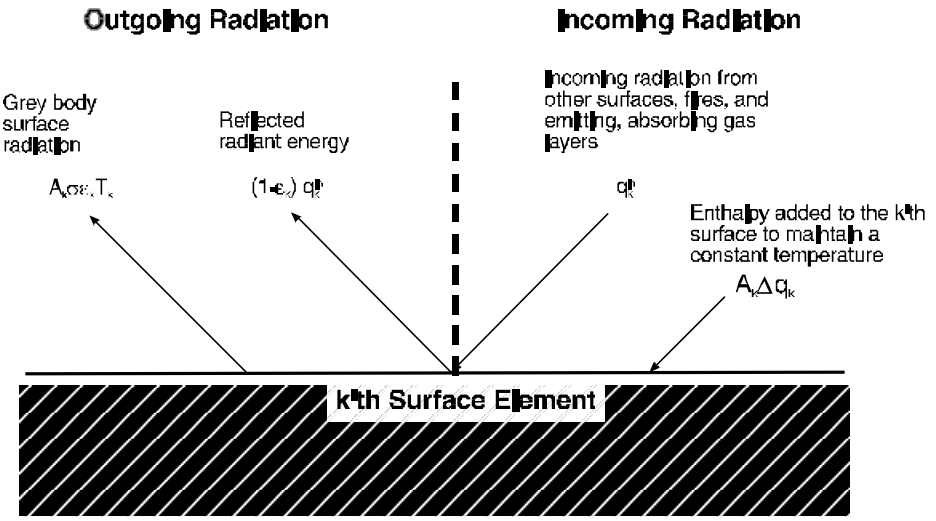

Figure 6. Radiation exchange in a two-zone fire model.

$$A_k \epsilon_k \sigma_k T_k^4 + (1-\epsilon_k) q_k'' = q_k'' + A_k \Delta q_k'' \quad (k = 1,..N). \tag{37}$$

Radiation exchange at each wall segment has emitted, reflected, incoming and net radiation terms. Equation (37) then represents a system of linear equations that must be solved for) q" to determine the net fluxes given off by each surface. The setup and solution of this linear system is the bulk of the work required to implement the net radiation method of Siegel and Howell. Equation (38) derived by Siegel and Howell [30] and listed there as eqs 17 to 20, is called the net radiation equation,

$$\frac{\Delta q_k''}{\epsilon_k} - \sum_{J=1}^{N} \frac{1-\epsilon}{\epsilon_j} \Delta q_j'' F_{k-j} \tau_{j-k} = \sigma T_k^4 - \sum_{j=1}^{N} \sigma T_j^4 F_{k-j} \tau_{j-k} - \frac{c_k}{A_k}. \tag{38}$$

where F is the Stefan-Boltzman constant, ϵ_k is the emissivity of the k'th wall segment, T_k is the temperature of the k'th wall segment, F_{k-j} a configuration factor, and J is a transmissivity factor. This latter is the fraction of energy passing unimpeded through a gas along a path from surface j to k. The parameters c_k represent the various sources of heat, namely the fire itself and the gas layers. In the form shown, the view factor of the k'th element is included in the parameter c_k.

The actual implementation uses a slightly modified form of eq (38), namely

$$\Delta q_k'' - \sum_{j=1}^{N} (1-\epsilon_j) \Delta q_j'' F_{k-j} \tau_{j-k} = \sigma T_k^4 - \sum_{j=1}^{N} \sigma T_j^4 F_{k-j} \tau_{j-k} - \frac{c_k}{A_k}, \text{ where} \tag{39}$$

$$\Delta q_k'' = \epsilon_k \Delta \hat{q}_k''. \tag{40}$$

There are two reasons for solving eq (39) rather than eq (38). First, since ϵ_k does not occur in the denominator, radiation exchange can be calculated when some of the wall segments have zero emissivity. Second and more importantly, the matrix corresponding to the linear system of eq () is diagonally dominant [29]. Iterative algorithms can be used to solve such systems more efficiently than direct methods such as Gaussian elimination. The more diagonally dominant a matrix (the closer the emissivities are to unity), the quicker the convergence when using iterative methods. Typical values of the emissivity for walls subject to a fire environment are in the range of $0.85 < \epsilon < 0.95$, so this is a reasonable approximation. The computation of, $F_{k\text{-}j}$, $J_{j\text{-}k}$ and c_k is discussed by Forney [29]. It is shown how it is possible to use the symmetries present in the four wall segment problem to minimize the number of direct configuration factor calculations required. In earlier versions of CFAST, the gas transmittance per unit length was assumed constant. In this new version, is calculated from the properties of the gas layers.

Transmissivity*:* The transmissivity of a gas volume is the fraction of radiant energy that will pass through it unimpeded and is given by

$$\tau(y) = e^{-ay} \tag{41}$$

where a is the absorptance per unit length of the gas volume and y is a characteristic path length.

In a two layer zone model, a path between an object (fire, wall segment, *etc.*) and a target may traverse through both layers. In this case, the length of the path in the lower layer, y_L, can be computed given the total distance S between the object and target, and the elevations of the target, y_t, object, y_o and layer, y_{lay}, to be

$$y_L = \begin{cases} 0, & y_{lay} < y_{min} \\ \dfrac{y_{lay} - y_{min}}{y_{max} - y_{min}} S, & y_{min} \le y_{lay} \le y_{max} \\ S, & y_{lay} \ge y_{max} \end{cases} \tag{42}$$

where

$$\begin{aligned} y_{min} &= \min(y_0, y_t) \\ y_{max} &= \max(y_0, y_t) \end{aligned}, \tag{43}$$

the path length in the upper layer is $y_U = S - y_L$, and the transmittance of the lower (upper) layer is denoted J_L (J_U).

Absorptivity: The absorptivity, α, of a gas volume is the fraction of radiant energy absorbed by that volume. For a grey gas $\alpha + \tau = 1$. The absorptivity of the lower (upper) layer is denoted α_L (α_U).

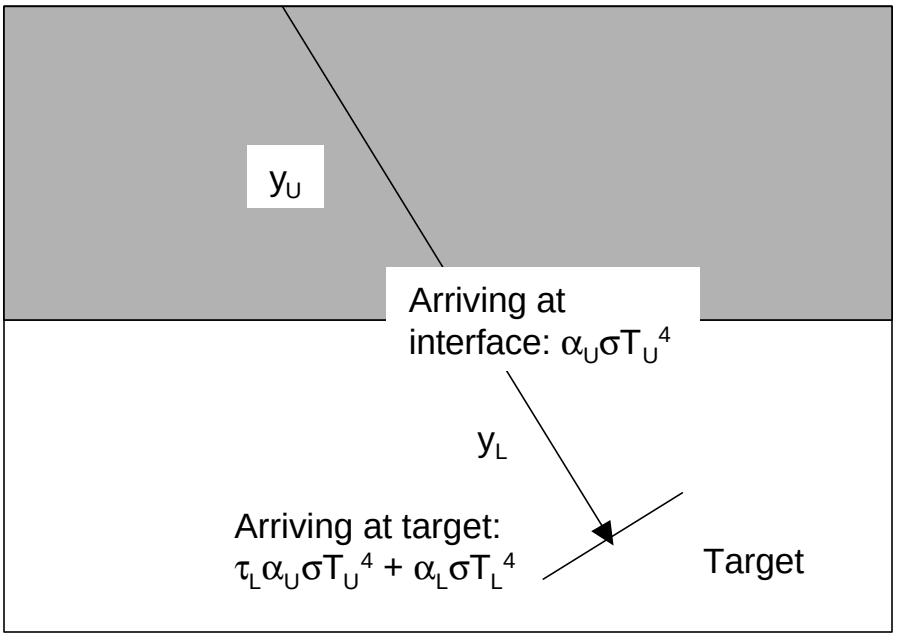

$\alpha_U = 1 - \exp(-a_U y_U)$ = emittance of upper layer

$\alpha_L = 1 - \exp(-a_L y_L)$ = emittance of lower layer

$\tau_L = \exp(-a_L y_L)$ = transmittance of lower layer

Figure 7. Radiative heat transfer from a wall surface in the upper layer to a target in the lower layer.

Inter-compartment Heat Transfer

Heat transfer between vertically connected compartments is modeled by merging the connected surfaces for the ceiling and floor compartments or for the connected horizontal compartments. A heat conduction problem is solved for the merged walls using a temperature boundary condition for both the near and far wall. As before, temperatures are determined by the DAE solver so that the heat flux striking the wall surface (both interior and exterior) is consistent with the temperature gradient at that surface.

For horizontal heat transfer between compartments, the connections can be between partial wall surfaces, expressed as a fraction of the wall surface. CFAST first estimates conduction fractions analogous to radiative configuration factors. For example, a conduction fraction between a rear

wall in room 1 and a front wall room 2 is the heat flux fraction from the room 2 wall that strikes contributes to room 1's wall heat transfer. Once these fractions are determined, an average flux, q_{avg}, is calculated using

$$q_{avg} = \sum_{walls} F_{ij} q_{wall_j}$$

where F_{ij} is the fraction of flux from wall i that contributes to wall j, q_{wallj} is the flux striking wall j

Ceiling Jet

Relatively early in the development of a fire, fire-driven ceiling jets and gas-to-ceiling convective heat transfer can play a significant role in room-to-room smoke spread and in the response of near-ceiling mounted detection hardware. Cooper [34] details a model and computer algorithm to predict the instantaneous rate of convective heat transfer from fire plume gases to the overhead ceiling surface in a room of fire origin. The room is assumed to be a rectangular parallelopiped and, at times of interest, ceiling temperatures are simulated as being uniform. Also presented is an estimate of the convective heat transfer due to ceiling-jet driven wall flows. The effect on the heat transfer of the location of the fire within the room is taken into account.

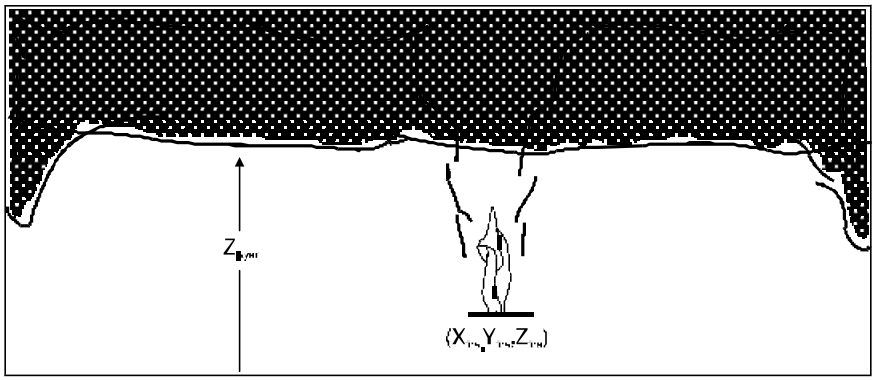

Figure 8. Convective heat transfer to ceiling and wall surfaces via the ceiling jet.

A schematic of a fire, fire plume, and ceiling jet is shown in Figure 8 The buoyant fire plume rises from the height Z_{fire} toward the ceiling. When the fire is below the layer interface, its mass and enthalpy flow are assumed to be deposited into the upper layer at height Z_{layer}. Having penetrated the interface, a portion of the plume typically continues to rise toward the ceiling. As it impinges on the ceiling surface, the plume gases turn and form a relatively high temperature, high velocity, turbulent ceiling jet which flows radially outward along the ceiling and transfers heat to the relatively cool ceiling surface. The convective heat transfer rate is a strong function of the radial distance from the point of impingement, reducing rapidly with increasing radius. Eventually, the relatively high temperature ceiling jet is blocked by the relatively cool wall surfaces [35]. The ceiling jet then turns downward and outward in a complicated flow along the vertical wall

surfaces [36], [37]. The descent of the wall flows and the heat transfer from them are eventually stopped by upward buoyant forces. They are then buoyed back upward and mix with the upper layer.

The average convective heat flux from the ceiling jet gases to the ceiling surface, $\dot{Q}_{ceil}$, can be expressed in integral form as

$$\dot{Q}_{ceil} = \int_0^{X_{wall}} \int_0^{Y_{wall}} \dot{q}''_{ceil}(x,y)\, dx dy \tag{45}$$

The instantaneous convective heat flux, $\dot{q}''_{ceil}(X,Y)$ can be determined as derived by Cooper [34]:

$$\dot{q}''_{ceil}(x,y) = h_l \left(T_{ad} - T_{ceil}\right) \tag{46}$$

where T_{ad}, a characteristic ceiling jet temperature, is the temperature that would be measured adjacent to an adiabatic lower ceiling surface, and h_l is a heat transfer coefficient. Reference [34] provides details of the calculation of wall surface area and convective heat flux for the wall surfaces.

Detection and Suppression

Only very simple suppression algorithms exist. Within the context of zone models, geometry factors have not been implemented. There are two reasons. The first is that computational, shadows require three-dimensional information. The second reason involves the effect the suppression system has on a fire. There are three types of suppression: deluge, chemical and mist. In all three cases, there is not sufficient understanding of the mechanisms that a zone model can do more that reduce the heat release rate as a function of the quantity of water or other suppressant. The situation is even more difficult for mist systems, where the fluid dynamics is critical. It is unlikely that zone models will be able to tackle this technology and understanding the effects of mist, and similar, systems will be the province of computational fluid dynamics.

Limitations

Zone Model and Transport Limitations

The basic assumption of all zone fire models is that each compartment can be divided into a small number of control volumes, each of which is internally uniform in temperature and composition.

The boundary between the two layers in a compartment is called the interface. It has generally been observed that buoyantly stratified layers form in the spaces close to the fire. While in an experiment the temperature can be seen to vary within a given layer, these variations are small compared to the temperature difference between the layers.

Beyond the basic zone assumptions, the model typically involves a mixture of established theory (e.g., conservation equations), empirical correlations where there are data but no theory (e.g., flow

and entrainment coefficients), and approximations where there are neither (e.g., post-flashover combustion chemistry) or where their effect is considered secondary compared to the "cost" of inclusion. An example of a widely used assumption is that the estimated error from ignoring the variation of the thermal properties of structural materials with temperature is small. While this information would be fairly simple to add to the computer code, data are scarce over a broad range of temperatures even for the most common materials.

Burning can be constrained by the available oxygen. However, this "constrained fire" is not subject to the influences of radiation to enhance its burning rate, but is influenced by the oxygen available in the compartment. If a large mass loss rate is entered, the model will follow this input until there is insufficient oxygen available for that quantity of fuel to burn in the compartment. The unburned fuel (sometimes called excess pyrolyzate) is tracked as it flows out in the door jet, where it can entrain more oxygen. If this mixture is within the user-specified flammable range, it burns in the door plume. If not, it will be tracked throughout the building until it eventually collects as unburned fuel or burns in a vent. The enthalpy released in the fire compartment and in each vent, as well as the total enthalpy released, is detailed in the output of the model. Since mass and enthalpy are conserved, the total will be correct. However, since combustion did not take place adjacent to the burning object, the actual mass burned could be lower than that specified by the user. The difference will be the unburned fuel.

An oxygen combustion chemistry scheme is employed only in constrained fires. Here user-specified hydrocarbon ratios and species yields are used by the model to predict concentrations. A balance among hydrogen, carbon, and oxygen molecules is maintained. Under some conditions, low oxygen can change the combustion chemistry, with a resulting increase in the yields of products of incomplete combustion such as CO. Guidance is provided on how to adjust the CO/CO_2 ratio. However, not enough is known about these chemical processes to build this relationship into the model at the present time. Some data exist in reports of full-scale experiments (e.g., reference [38]) which can assist in making such determinations.

The entrainment coefficients are empirically determined values. Small errors in these values will have a small effect on the fire plume or the flow in the plume of gases exiting the door of that compartment. In a multi-compartment model such as CFAST, however, small errors in each door plume are multiplicative as the flow proceeds through many compartments, possibly resulting in a significant error in the furthest compartments. The data available from validation experiments [39] indicate that the values for entrainment coefficients currently used in most zone models produce good agreement for a three-compartment configuration. More data are needed for larger numbers of compartments to study this further.

In real fires, smoke and gases are introduced into the lower layer of each compartment primarily due to mixing at connections between compartments and from the downward flows along walls (where contact with the wall cools the gas and reduces its buoyancy). Doorway mixing has been included in CFAST, using the same empirically derived mixing coefficients as used for calculating fire plume entrainment. Downward wall flow has not been included. This could result in underestimates of lower layer temperatures and species concentration.

At the present time it is not practical to adapt currently available fire growth models for direct solution. Such data can be obtained by measurements taken in large- and small-scale calorimeters, or from compartment burns. Potential sources of uncertainty include measurement errors related to the instrumentation and the degree to which "free-burning" conditions are not achieved (e.g., radiation from the gases under the hood or from the hood itself, and restrictions in the air entrained by the object causing locally reduced oxygen concentrations affecting the combustion chemistry). There are limited experimental data for upholstered furniture which suggest that prior to the onset of flashover in a compartment, the influence of the compartment on the burning behavior of the item is small. The differences obtained from the use of different types or locations of ignition sources have not been explored. These factors are discussed in reference [40].

When small-scale calorimeter data are used, procedures are available to extrapolate to the behavior of a full-size item. These procedures are based on empirical correlations of data which exhibit significant scatter, thus limiting their accuracy. For example, for upholstered furniture, the peak heat release rates estimated by the "triangular approximation" method averaged 91 % (range 46 to 103 %) of values measured for a group of 26 chairs with noncombustible frames, but only 63 per cent (range 46 to 83 %) of values measured for a group of 11 chairs with combustible frames [41]. Also, the triangle neglects the "tails" of the curve; these are the initial time from ignition to significant burning of the item, and the region of burning of the combustible frame, after the fabric and filler are consumed.

Current Available Models

The following models either have a significant number of users or are currently supported. The list only includes zone models which are based on implementations of the conservation equations of mass and energy.

ASET - US
BRI2 - Japan
CFAST, FAST - US
CFIRE-X - Germany/Norway collaboration
CiFi - France
COMPBURN - US
COMPF2 - US
DSLAYV - Sweden
FIRST (HARVARD V) - US
FISBA - France
MAGIC - France
NRCC 1 and 2 (a component of FIRECAM) - Canada
RADISM - UK
RVENT - Norway
Sfire - Sweden

This list excludes models such as FPETool which are tools based on correlations, and specific application tools such as ASCOS and Contam, which (in this case) are for designing smoke control

systems. An important consideration in choosing one of these models for use is transparency of the methods used and the care with which the documentation has been prepared.

As can be seen from the discussion, the zone model concept covers a wide variety of phenomena. They are well suited to investigating most effects of fires in buildings. The caveat is that when detailed information about a flow field or temperature distribution is needed, use of a more detailed model as provided by computational fluid dynamics is required. For most other situations, though, the ability to model whole building systems provides a level of detail which is sufficient.

In most of the models in use today, there has been an effort at verification and validation. These efforts have focused on one or two aspects of each model, and a more complete treatise is awaiting development of the mathematics[42].

References

[1] Friedman, R., "Survey of Computer Models for Fire and Smoke," *Factory Mutual Research Corp.*, Norwood, MA, 02062 1990.

[2] Cooper, L.Y., "A Mathematical Model for Estimating Available Safe Egress Time in Fires," *Fire and Materials.* 1982, *6(4),* 135-144.

[3] Babrauskas, V., "COMPF2-A Program for Calculating Post-Flashover Fire Temperatures," *Natl. Bur. Stand. (U.S.)* 1979, *Tech. Note 991*, 76 p.

[4] Davis, W. D. and Cooper, L. Y., "Computer Model for Estimating the Response of Sprinkler Links to Compartment Fires With Draft Curtains and Fusible Link-Actuated Ceiling Vents," *Fire Technology* 1991, *27 (2),* 113-127.

[5] Tanaka, T., "A Model of Multiroom Fire Spread," *Nat. Bur. Stand. (U.S.)* 1983, *NBSIR 83-2718*, 175 p.

[6] Jones, W. W., A Multicompartment Model for the Spread of Fire, Smoke and Toxic Gases, Fire Safety Journal *9*, 55 (1985); Jones, W. W. and Peacock, R. D., Refinement and Experimental Verification of a Model for Fire Growth and Smoke Transport, Proceedings of the 2nd International Symposium on Fire Safety Science, Tokyo (1989); Jones, W. W. and Peacock, R. D., "Technical Reference Guide for FAST Version 18" Natl. Inst. Stand. Techol. Tech. Note 1262 (1989).

[7] Forney, G. P. and Cooper, L. Y., The Consolidated Compartment Fire Model (CCFM) Computer Application CCFM.VENTS - Part II: Software Reference Guide, Nat. Inst. Stand. Technol., NISTIR 90-4343 (1990).

[8] Jones, W. W. and Forney, G. P. "A Programmer's Reference Manual for CFAST, the Unified Model of Fire Growth and Smoke Transport," *Natl. Inst. Stand. Technol.* 1990, *Tech. Note 1283*, 104 p.

[9] Mitler, H. E. “Comparison of Several Compartment Fire Models: An Interim Report,” *Natl. Bur. Stand. (U.S.)* 1985, *NBSIR 85-3233*, 33 p.

[10] Jones, W. W. “A Review of Compartment Fire Models,” *Natl. Bur. Stand. (U.S.)* 1983, *NBSIR 83-2684*, 41 p.

[11] Cooper L. Y. and Forney, G. P., The consolidated compartment fire model (CCFM) computer application CCFM-VENTS – part I: Physical reference guide. Natl. Inst. Stand. Technol., NISTIR 4342 (1990).

[12] Forney, G. P. and Moss, W. F., Analyzing and Exploiting Numerical Characteristics of Zone Fire Models, Natl. Inst. Stand. Technol., NISTIR 4763 (March 1992).

[13] Jones, W. W. and Bodart, X., Buoyancy Driven Flow as the Forcing Function of Smoke Transport Models, Natl. Bur. Stand. (U. S.), NBSIR 86-3329 (1986).

[14] Rehm, R. G. and Forney, G. P., “A Note on the Pressure Equations Used in Zone Fire Modeling,” Natl. Inst. Stand. Technol., NISTIR 4906 (1992).

[15] Babrauskas, V., "Development of the Cone Calorimeter - A Bench Scale Heat Release Rate Apparatus Based on Oxygen Consumption," *Fire and Materials 8*, 1984, p 81.

[16] Thornton, “The Relation of Oxygen to the Heat of Combustion of Organic Compounds,” Philosophical Magazine and J. of Science, **33** (1917).

[17] Huggett, C., “Estimation of the Rate of heat Release by Means of Oxygen Consumption,” J. of Fire and Flammability, **12**, pp. 61-65 (1980).

[18] Standard Test Method for Heat and Visible Smoke Release for Materials and Products Using and Oxygen Consumption Calorimeter, ASTM E1354-90, *American Society for Testing and Materials*, Philadelphia, PA 1990.

[19] Standard Test Method for Heat and Visible Smoke Release for Materials and Products Using and Oxygen Consumption Calorimeter, ASTM E1354-90, American Society for Testing and Materials, Philadelphia, PA (1990).

[20] Morehart, J. H., Zukowski, E. E. and Kubota, T., Characteristics of Large Diffusion Flames Burning in a Vitiated Atmosphere, Third International Symposium on Fire Safety Science, Edinburgh (1991).

[21] Quintiere, J. G., Steckler, K., and Corley, D., An Assessment of Fire Induced Flows in Compartments, Fire Science and Technology *4*, 1 (1984).

[22] Quintiere, J. G., Steckler, K. and McCaffrey, B. J., "A Model to Predict the Conditions in a Room Subject to Crib Fires," First Specialist Meeting (International) of the Combustion Institute, Talence, France 1981.

[23] Cooper, L. Y., Calculation of the Flow Through a Horizontal Ceiling/Floor Vent, Natl. Inst. Stand. Technol., NISTIR 89-4052 (1989).

[24] Klote, J.K. and Milke, J.A., Design of Smoke Management Systems, American Society of Heating, Refrigerating and Air-conditioning Engineers, Atlanta, GA (1992).

[25] ASHRAE Handbook HVAC Systems and Equipment, American Society of Heating, Refrigerating and Air-Conditioning Engineers, Atlanta, GA (1992).

[26] Klote, J. H., A Computer Model of Smoke Movement by Air Conditioning Systems, NBSIR 87-3657 (1987).

[27] 1989 ASHRAE Handbook Fundamentals, American Society of Heating, Refrigeration and Air Condition Engineers, Inc., Atlanta, GA 1989.

[28] McGrattan, K. B., Baum, H. R., and Rehm, R. G., Large Eddy Simulations of Smoke Movement, Fire Safety J. **30** (2), pp 161-178 (1998).

[29] Forney, G. P., Computing Radiative Heat Transfer Occurring in a Zone Fire Model, Natl. Inst. Stand. Technol., NISTIR 4709 (1991).

[30] Siegel, R. and Howell, J. R., Thermal Radiation Heat Transfer, Hemisphere Publishing Corporation, New York, second ed. (1981).

[31] Hottel, H. C., Heat Transmission, McGraw-Hill Book Company, New York, third ed. (1954).

[32] Hottel, H. and Cohen, E., Radiant Heat Exchange in a Gas Filled Enclosure: Allowance for non-uniformity of Gas Temperature, American Institute of Chemical Engineering Journal *4*, 3 (1958).

[33] Yamada, T. and Cooper, L. Y., Algorithms for Calculating Radiative Heat Exchange Between the Surfaces of an Enclosure, the Smoke Layers and a Fire, Building and Fire Research Laboratory Research Colloquium, July 20, 1990.

[34] Cooper, L. Y., Fire-Plume-Generated Ceiling Jet Characteristics and Convective Heat Transfer to Ceiling and Wall Surfaces in a Two-Layer Zone-Type Fire Environment, Natl. Inst. Stand. Technol., NISTIR 4705, 57 p. (1991).

[35] Cooper, L. Y., Heat Transfer in Compartment Fires Near Regions of Ceiling-Jet Impingement on a Wall. J. Heat Trans., 111, pp. 455-460 (1990).

[36] Cooper, L. Y., Ceiling Jet-Driven Wall Flows in Compartment Fires. Combustion Sci. and Technol., 62, pp. 285-296 (1988).

[37] Jaluria, Y. and Cooper, L. Y., Negatively Buoyant Wall Flows Generated in Enclosure Fires. Progress in Energy and Combustion Science, 15, pp. 159-182 (1989).

[38] Lee, B.T., "Effect of Ventilation on the Rates of Heat, Smoke, and Carbon Monoxide Production in a Typical Jail Cell Fire," Natl. Bur. Stand. (U.S.), NBSIR 82-2469, 1982.

[39] Peacock, R. D., Davis, S., Lee, B. T., "An Experimental Data Set for the Accuracy Assessment of Room Fire Models," Natl. Bur. Stand. (U.S.), NBSIR 88-3752, April 1988, p. 120.

[40] Babrauskas, V., Lawson, J. R., Walton, W. D., Twilley, W. H., "Upholstered Furniture Heat Release Rates Measured with a Furniture Calorimeter," Natl. Bur. Stand. (U.S.), NBSIR 82-2604, 1982.

[41] Babrauskas, V. and Krasny, J. F., "Fire Behavior of Upholstered Furniture," Natl. Bur. Stand. (U.S.), Monogr. 173, 1985.

[42] Quantifying Fire Model Evaluation Using Functional Analysis, Fire Safety Journal, *33*, 167-184, 1999, Peacock, R. D.; Reneke, P. A.; Davis, W. D.; Jones, W. W.